Predicted Burning Rates of Single Carbon Particles

Robert H. Essenhigh, Robert Froberg
and Jack B. Howard

Department of Fuel Technology
The Pennsylvania State University
University Park, Pennsylvania

1. INTRODUCTION

In spite of the immense amount of research on combustion of carbon in the last 30 years, the classic experiments of Tu, Davis, and Hottel (1) on 1" spheres are still of the best, and perhaps still the most widely quoted, of all experimental work on the subject, carried out at atmospheric pressure, and in this range of particle size and temperatures. The theory, of course, has advanced in several particulars since then (see Reviews (2-5)) and it has long been known that the original Tu et al. theoretical analysis was inadequate. In the original analysis, only desorption and boundary layer diffusion were considered as possible rate-controlling steps in the reaction: chemisorption and internal reaction were neglected. This neglect was simply that, at that time of writing, these two latter concepts had not been formulated, or not generally accepted; also, as a bias against considering adsorption, this was always assumed to be so fast as to be effectively instantaneous. According to Brunauer (6), the concept of activated adsorption was first formulated in the early 1930's - about the time of writing of the Tu et al. paper, or soon after - but, even a decade later, it still had not been generally accepted, with the consequence that many true chemisorption processes even then were being incorrectly interpreted in terms of solution, diffusion, migration (mobile adsorption), or reaction at the solid surface itself (6). Analysis of the internal reaction processes came even later, and has only been developed in the last decade or so.

Thirty years of research, therefore, has largely inverted the relation between theoretical to experimental work: that is to say, theory now leads experiment in consolidated development. Even so, the theoretical position is still confused: confidence in many of the theoretical concepts is still low as there are now almost too many theoretical possibilities available to explain any given set of new experimental data. Further definitive experiments are required to clarify quite a number of theoretical ambiguities, inconsistencies, and contradictions. One particular such point of major fundamental and practical concern at the present moment is the relative importance of the three principal "resistances" (1,7) in the carbon oxidation reaction. The three resistances are those of: boundary layer diffusion (S_0); adsorption (S_1); and desorption (S_2). For many years, only diffusion was ever considered as the rate control at temperatures in excess of 1000°K. Hottel and Stewart (8) had in fact shown conclusively, 25 years ago, that this was definitely not the case for small particles of pulverised-coal size, in flames, but little or no notice seems to have been taken of this paper till recently. Latest work, (9,10) however, has now confirmed the essential correctness of Hottel and Stewart's conclusion, but this now brings in question the basis of the previous belief, and also over what range of particle sizes and temperatures the new conclusion is valid.

In support of the original contention of diffusional control at high temperatures, the paper most frequently quoted would seem to have been that of Tu et al. Since, however, the original analysis was incomplete or inadequate, for the reasons given above, our thought was that the Tu et al. data might not be inconsistent with the new concepts, but simply had never been tested against them. It is true that their data apparently gave full support to the concept of diffusion control, but it has been shown elsewhere (2) (following Brunauer's (6) suggestion), that many combustion data can reasonably be reinterpreted in terms of an activated adsorption control, instead of the generally assumed diffusion control - if it can be accepted that the activation energy, though low, is finite, in the region of 2000 to 4000 cal., and therefore able to generate a small, but not negligible, resistance. Given this assumption, the Tu et al. data can then, apparently, be shown to give equally full support to the alternative hypothesis of adsorption control. This evident contradiction (i.e., equal support to both hypotheses(, means of course, that the intrepretation of the data, as analysed to date, is ambiguous; but it seemed to us, nevertheless, that the ambiguity was in the analysis, not in the data. Therefore, if the data were of the high quality that is generally claimed for them, it might be possible to remove the ambiguities by using the data to test the full equations now available in the literature (3-5), instead of the partial equations used hitherto (1) (see also (11,12)) which were generally based on unverified assumptions of very rapid, and therefore neglectable, adsorption.

The purpose of this paper, therefore, is to present this re-analysis It shows that the data are indeed of excellent quality (thus eliminating the need for repeat of the experiments). It also shows that adsorption presents a small, but significant resistance, which increases in importance as the particle size drops, becoming dominant at something under 100 microns. There are, therefore, no essential inconsistencies with other and more recent data, so the tested equations can be used to some extent to predict combustion behaviour of very small particles.

2. THEORY

The literature and general theory of carbon combustion has been reviewed so often, and so extensively (2-5), in the last few years, that we do not intend, in this section, to do more than set out the essential equations in the best form for our immediate purpose of testing them by re-analysis of the Tu et al. (1) experimental data. The most exhaustive of the reviews is that by Walker et al. (4) who paid particular attention to mechanism details, internal reaction, CO_2 and other reactions, and influence of radiation. For our purposes here, however, the nomenclature of the other reviews is more convenient, and has therefore been followed.

2.1 General Model - The classic picture of heterogeneous reaction between a flowing fluid and the solid it surrounds (e.g., (13,14)) is that of a three stage process. (1) The reacting fluid diffuses through a boundary layer against the counter diffusion of inerts and/or reaction products - e.g., N_2, CO_2, CO. (2) At the solid surface the reacting fluid is chemisorbed, requiring activation energy of adsorption, E_1. (3) After a finite residence time, which can be microseconds, the final reaction step is completed with the desorption of the adsorbed material which carries with it the underlying atom of the solid, so forming the reaction products: this requires activation energy, E_2. The total process is then completed with counter-diffusional escape of these products into the main fluid stream. This general process can then be treated mathematically by setting up the simultaneous equations both for boundary layer and pore diffusion and for the appropriate adsorption isotherms. These are the subjects of the next two section.

2.2 Diffusion - Potentially, this can operate in two ways: by boundary layer (external) diffusion; and by pore (internal) diffusion.

(i) Boundary layer diffusion: The existence of this process is well established, and the process well understood; and, as a result of excellent agreement between prediction and experiment (15-17), confidence in the absolute accuracy of the diffusion calculations for combustion rates is now high.

To treat diffusion mathematically, we define a velocity constant for mass transfer (transfer coefficient), k_o, by the equation:

$$R_s = k_o(p_o - p_s) \tag{1}$$

where p is the oxygen partial pressure, with subscripts o and s for values, respectively: in the main stream, and adjacent to, the solid surface. The velocity constant, k_o, is a function of particle size and general ambient conditions, including temperature and velocity in particular. Standard analysis of this system, following Nusselt (14), leads to an equation for k_o that may be written as the temperature function:

$$k_o = A_o(T/T_o)^{n-1} \tag{2}$$

where A_o is a velocity dependent coefficient, given below; and n is an index generally lying between 1.5 and 2, depending on the nature of the diffusing gases involved. For oxygen in nitrogen, which is the dominant system in air-combustion, experiment gives the best value for n as 1.75 (18,19). The coefficient A_o is given by:

$$A_o = (\rho_o M_c/M_o)\ (D_o/d)\,Nu = K.Nu \tag{3}$$

where ρ_o is the s.t.p. density of oxygen; M_c and M_o are the molecular weights of carbon and oxygen respectively; D_o is the s.t.p. diffusion coefficient of oxygen through nitrogen; d is the particle diameter; and Nu is the Nusselt number for mass transfer. In general, Nu is a function of the Reynolds and Prandtl numbers that can be written

$$Nu = 2 + c.Re^m.Pr^n \tag{4a}$$

where c is a numerical constant, ranging in value (according to both the heat and the mass transfer literature (20,21)) from 0.18 to 0.7, obtained by correlation of data. Grober and Erk (20), in their review of the mass transfer data, give only the one value of 0.6 (22). This is close to Khitrin's value of 0.7 (23), quoted by Golovina and Khaustovich (24). The Pr index, n, is given by nearly all as 1/3, but in any case the Prandtl number in this instance is so close to unity that its cube root can be taken as 1 with less than 1% error. The Re index, m, is also given a range of values, from 0.5 to 0.8 (see (20,21)) in the heat transfer literature, but again, the purely mass transfer literature seems to agree on 1/2. This is given by Ranz and Marshall (22) and by Khitrin, (23) and it is also the value used to correlate combustion data by Graham et al. (25) and by Day (26). Walker et al. (4) do quote lower coefficients than this for various combustion systems, but the systems are not isolated spheres. Taking the value of 0.6 for c, 1/2 for m, unity for Pr, and expanding the Reynolds number into a coefficient and a velocity, we can rewrite eqn (4a) as:

$$Nu = 2 + c'.v_o^{1/2} \tag{4b}$$

where c' takes the value: 2.64 (at c = 0.6).

(ii) Pore diffusion: This potentially can play a part only in the event of pore or internal reaction. If it does so, however, it has been shown

elsewhere (27,5) that its effect is to generate modified velocity constants for the adsorption and desorption processes. This means that the equations to be developed in the next section (2.3) are potentially capable of accounting for pore reaction as they stand, with the sole modification of using apparent velocity constants in place of the true ones, with auxiliary equations to relate the true and effective constants. These modified and auxiliary equations are given in the literature (4,5,27), but we are not giving them here since, to anticipate our conclusion, we found no apparent or detectable influence of pore diffusion. This was not entirely unexpected since the burn-off on the whole was fairly low, and little development of internal surface would have had time to take place. An indicator to this result was also provided by the original conclusion of Tu et al. (1) that the low temperature reaction was zero order, with respect to the oxygen partial pressure, whereas this would have been a half order reaction had internal diffusion played a part.

We therefore saw no point in quoting the pore diffusion equations. We mention it here only to show that the point was considered and capable of being incorporated.

2.3 Adsorption Isotherm - (i) Basis of choice: To set up the equation for the reaction process itself requires first the selection of an appropriate isotherm. Our choice here has been made partly on the basis of the behaviour of the most likely isotherms and manipulation of the resulting equations, and partly on the basis of Occams Razor (the Principle of Minimum Hypotheses).

The two isotherms considered were the Langmuir and the Temkin isotherms. Ideally, selection of an isotherm should be carried out by experiments to test and determine the most probable one, but this has not yet been done for this system. In general, however, the literature shows that most experimental data have been correlated on the basis of a Langmuir isotherm (28,29,30).

Information based on the variation of activation energies is also inconclusive. If a Temkin isotherm is involved, these energies must change with percentage coverage of the solid surface by the adsorbed layer. Data on these energies, however, are only plentiful for the desorption process; for the adsorption process they are very scarce. For desorption, the literature (3,4,21,30) gives values ranging from 20,000 to 80,000 cal.; but these seem principally to vary with the experimental system, and with the type of carbon used: the changes are never explicitly attributed to change of percentage coverage. For adsorption, it has already been mentioned in the Introduction that the value is expected to be low. This is the summary conclusion by Trapnell (31) in view of the speed and ease of chemisorption at normal and low (-70°C) temperatures. Trapnell also quotes values from Barrer (32) which start at 4000 cal. at low coverage, in agreement with Blyholder and Eyring's figure (30), and also in agreement with the re-estimates (2) of data in the literature. Barrer also shows that the value rises with coverage, the highest figure he found being 23,000 cal. At this degree of coverage, however, the activation energies are approaching those of desorption, and it will be shown below (Analysis sec. 3.3) that the effects of rising E_1 and falling E_2 with increasing coverage do in fact offset each other: the actual degree to which this occurs can only be determined by experiment, and this has never been done. This occurs in the middle range of the isotherm. At the extreme limits, at high and at low coverage, the two isotherms in any event tend toward each other, so the offsetting effect of changing E_1 and E_2 in the middle region of coverage will tend to restore a Temkin isotherm at least to a pseudo-Langmuir isotherm. Since the use of a Temkin isotherm renders the equations somewhat intractable, and in any event has never been conclusively established, we therefore decided to use the Langmuir isotherm (on the basis of Occams Razor) since this involved fewer and simpler assumptions, though this use was still with the reservation that, if such an isotherm could be used successfully, it might still be only a pseudo-isotherm.

(ii) Langmuir isotherm: This isotherm depends on only two velocity constants: one for the adsorption process, k_1; and one for the desorption process, k_2. Both are assumed to be invariant with respect both to oxygen concentration, and to percentage coverage of the solid surface by the adsorbed film. If the specific reaction rate is R_s (gm of carbon/sq. cm. sec.), the Langmuir isotherm then gives us (5)

$$1/R_s = (1/k_1 p_s) + (1/k_2) \tag{5}$$

where p_s is the oxygen concentration adjacent to the solid carbon surface. The velocity constants can be written in general as

$$k_1 = A_1 . \exp(-E_1/RT) \tag{6a}$$

$$k_2 = A_2 . \exp(-E_2/RT) \tag{6b}$$

where the E's are the activation energies as already defined; and A_1 and A_2 are the pre-exponential constants or frequency factors. Like E_1 and E_2, A_2 can only be determined experimentally for the particular system under consideration; but A_1 can, in principle, be calculated from Kinetic Theory, which gives

$$A_1 = B_1/\sqrt{T/T_o} \tag{7a}$$

and

$$B_1 = M_c P \eta/\sqrt{2\pi MRT_o} \tag{7b}$$

where: P is the absolute total pressure (dynes/sq.cm.); M is the mean molecular weight of the ambient gas; R is the gas constant; and η is a steric, orientation, or entropy factor for the oxygen as it is adsorbed on the solid surface.

For reasons to be explained below (Analysis, sec. 3), it is convenient to incorporate the root-temperature term in an apparent or effective activation energy E_1', whence we may write

$$k_1 = B_1 . \exp(-E_1/RT)/\sqrt{T/T_o} \tag{8a}$$

$$= B_1' . \exp(-E_1'/RT) \tag{8b}$$

The objective of this is to reduce the temperature-dependent factor A_1 to a temperature-independent factor B_1, and hence to B_1', ($=B_1/b$, where $b = 3.9$), where the factors B are also independent of velocity.

2.4 Combined Kinetics - To take all the possible factors into account simultaneously, it is clear that we must set up the equation for the combined kinetics by elimination of the unknown partial pressure p_s by solving for this between eqns (1) and (5) and equating. This gives the quadratic:

$$R_s^2 - (k_o p_o + k_2 + k_o k_2/k_1) R_s + (k_o p_o) k_2 = 0 \tag{9}$$

This is already cumbersome: it is clear that if the expressions for the velocity constants (k) are also inserted, the equation becomes totally unweildly. There are then so many coefficients that the expression could be fitted to anything at all, relevant or not. For this reason, we have tried, in our Analysis (sec. 3, below) to consider special cases that can be legitimately extracted, and to test the expression, unit by unit. For this reason we derive two of the special cases of importance, in this section, for use in the analysis below.

(i) k_2 large: For this special case, we divide the equation through by k_2 and, find that, when k_2 is large, the two terms (R_s^2/k_2) and $(k_o p_o/k_2)$ both become vanishingly small.[2] This leaves only the familiar "resistance" equation:

$$1/R_2 = (1/k_o p_o) + (1/k_1 p_o) \quad (10a)$$

$$= S_o + S_1 \quad (10b)$$

where 'S' is the appropriate resistance.

The significant point of this equation is that the reaction rate is first order (proportional to p_o) whatever the relative values of k_o and k_1. This is important as this resistance equation applies only when k_2 is large, i.e., at high temperatures. This was the central error of the original Tu et al. (1) analysis since the authors started by assuming that the reaction was first order, over the whole temperature range; they then showed experimentally that the first order reaction was true only above 1100 or 1200°K, with a zero order reaction below this temperature (as later confirmed by others (33,34)); but yet they continued to analyse the full data in terms of their only-partially applicable equations. For these reasons, the activation energy was mis-identified, and the part played by adsorption in the high temperature region was not appreciated.

(ii) k_1 large: The original Tu et al. analysis therefore was based on the concept of full chemical control at low temperatures, and full diffusional control at high temperatures. This only follows if adsorption is so fast that k_1 is very large, and we than have another special case of great interest. For k_1 large, the term $(k_o k_2/k_1)$ in eqn. (9) vanishes, and the resulting expression then factorises:

$$(R_s - k_2)\ (R_s - k_o p_o) = 0 \quad (11)$$

What this implies is that: k_2 is controlling at low temperatures; $k_o p_o$ is controlling at high temperatures; but, between the two, there is no transition region. Change from one region to the other is quite discontinuous. There is, of course, continuity in the reaction rate values; but there is complete discontinuity in the slopes of the two curves at the junction of the two regions. Experimentally, this has been shown explicitly for the carbon-hydrogen reaction (35), and implicitly for the carbon-oxygen reaction under such conditions that the reaction is possibly that by CO_2, with the carbon, in a double film at the onset of diffusion (24).

(iii) k_o large: For this condition, inserted for completeness, eqn. (9) reduces to the Langmuir isotherm of eqn. (5), though with p_o substituted for p_s. We can then write in the resistance notation:

$$1/R_s = S_1 + S_2 \quad (5a)$$

3. ANALYSIS

In this analysis, now to be developed below, our essential objective was to extract experimental values, from the experimental data, in such a form that it would then be possible to check one dependent variable against one independent one, according to the developed equations, all other variables remaining constant in the particular process being checked. This seemed to us to be the only valid way of testing such involved and elaborate equations as those given above, though it is conceded that the methods of extracting the operating values may perhaps be regarded as somewhat questionable in one or two particulars. However, it is difficult to see what other approach could have been adopted.

The analysis starts with a re-presentation of the data.

3.1 Data Plot - Fig. 1 shows the plot of the original Tu, Davis, and Hottel data (1), but as an Arrhenius plot instead of the double-log plot that they used; also using carbon surface temperatures as being more relevant then furnace temperature.

On this plot, the almost-vertical dotted line on the right is the k_2 term, fitted to the data, with an activation energy (E_2) taken as 40,000 cal. This value was selected as it gave a better fit to the data than the 35,000 cal. quoted by the original authors; it was also closer to other values found for electrode carbon (see (3,4,21)).

The heavy lines are "back-plots" calculated according to eqn. (9) using values of the constant coefficients as determined by this analysis.

3.2 Empirical Correlation - If the calculated back-plots of Fig. 1 are carefully compared with the original curves drawn in the original Tu et al. paper, which latter were drawn empirically, the two sets will be seen to follow each other very closely. This agreement was quite fortuitous, but it so happened that the original curves were of considerable assistance in providing us with a starting point in the analysis. In the first place, the marked curvature of the lines in the original plot showed that the limiting approximation of eqn. (11) clearly did not apply. Therefore, if any approximation applied, it would be closer to a Langmuir isotherm; moreover, this expectation was strongly supported by the shape of the curves. These all have a common starting point at low temperatures, with "fine-structure" splitting at high temperatures due to both oxygen concentration, and velocity. What, therefore, we had to investigate was the possibility that the curves were modified Langmuir isotherms, obeying a two-term equation of the form:

$$1/R_s = 1/k_2' + 1/k_2 \qquad (12)$$

where k_2 is identified from the start with the same k_2 desorption step as in the previous equations; but k_2' is inserted empirically. This is initially defined, also empirically, by:

$$k_2' = A_2'.\exp(-E_1'/RT) \qquad (13)$$

where E_1' is an effective activation energy that is identified below as the E_1' of eqn. (8b), and so is written as such here; and A_2' is an empirical velocity and concentration-dependent coefficient or frequency factor.

Our procedure now is: first, to show that this formulation has empirical value in correlating the data, to reduce these to specifications in terms of empirical equations, incorporating empirical definitive, coefficients; and secondly, to show that the empirical definitive coefficients also have fundamental justification and meaning.

3.3 Data Fit - To correlate the data by means of eqn. (12), the method used is illustrated in Fig. 2. This illustrates the method for just three of the data sets: namely, for the three oxygen concentrations, 21.0%, 9.69%, and 2.98%, at the single approach velocity of 3.51 cm./sec. All the other data were treated similarly (plots not reproduced). On these data plots, two "fitting" lines were drawn, one equivalent to a slope of 2,000 cal., for E_1', and the other equivalent to a slope of 40,000 cal., for E_2. Parallel to these two lines, further lines were drawn which were expected to be the limiting assymototes of the "Langmuir" curves when these were calculated and drawn in on top of the data. For the data of Fig. 2, this gave us, as can be seen, four such fitted lines, three for the slopes of E_1', and one for the slope of E_2.

As mentioned above, the k_2 line was retained as common to all the data (common A_2 and E_2), for all velocities and oxygen concentrations, but there were nine different values obtained of the empirical frequency factor A_2', though at the common value of 2,000 cal. for E_1. This splits the data into temperature-dependent, and temperature-independent groups or coefficients (i.e., exp(-E/RT) and A).

Once the k_2 and k_2' lines had been drawn in, the "Langmuir" curves were easily calculated and drawn in, as shown in Fig. 2. Because this was an empirical procedure, several tries were required for some of the lines to get a placing of the k_2' line that would give the best looking fit (by eye) of the Langmuir curves to the experimental data. In this fitting process, a value of 4,000 cal. was also tried for E_1', but the fit given was very poor in comparison to the finally-adopted value of 2000 cal. Two other values for E_2 were likewise tried: 35,000 cal. as proposed by Tu et al., and 58,000 cal. as proposed by Wicke (36). It was found by this that, within the limits of the experimental scatter, the fitted curves were somewhat insensitive to increase of E_2 above 40,000 cal. (the value finally selected), but the finally selected value seemed to be the best compromise between the slightly conflicting demands of all the data sets. It can also be seen, however, on both Fig. 1 and 2, that the final Langmuir curve has a long traverse at the lower temperatures, particularly for the 50.0 cm./sec. line at 21% oxygen, that has very little curvature and, within little error, a straight line could be drawn in, as an approximation, that would have an effective slope of close to 35,000 cal. This would appear to be the origin of Tu et al's figure of 35,000, and therfore substantiated our conclusion that our value should exceed theirs.

One final point can also be illustrated on Fig. 2. If we accept that the value of E_1 will rise, and E_2 will drop, with increasing surface coverage, (i.e., decreasing temperature), the effect is shown in Fig. 2 by the dotted curved lines. It is quite clear from this that, in plotting out the composite Langmuir curve, the two tendencies could very well offset each other, as described above, thus restoring what might be a Temkin isotherm to a pseudo-Langmuir isotherm. This helps to justify our procedure, at least from the empirical point of view.

3.4 Identification - The procedure outlined above demonstrates that the data can be described, to some degree of accuracy, by eqn. (12), with the k_2 and k_2' components described by eqns. (6b) and (13). Now, if the experiments had all been carried out at temperatures in excess of about 1100°K, and had been continued to higher temperatures still, the k_2 term would have been relatively unimportant, and the data could have been described empirically by the k_2' term alone. If, therefore, we now concentrate solely upon the k_2' term, what our fitting procedure has done is to correct the data for the k_2 component, and it now allows us to treat the data as if the k_2 term were very large - i.e., the low temperature resistance, S_2, is very small. But, under these circumstances, the original eqn. (9) reduces to the familiar resistance approximation of eqn. (10), which can be written in the alternative form:

$$R_s = k_1 p_1 / (1 + k_1/k_o) \quad \text{(for } k_2 \text{ large)} \qquad (14)$$

and this can now be compared with the empirically derived equation:

$$R_s = k_2' = A_2' . \exp(-E_1'/RT) \qquad (15)$$

this being the contraction of eqn. (12) when k_2 is very large. The A_2' coefficients are temperature independent, but still concentration and velocity dependent. If, therefore, the empirical coefficients A_2' have any fundamental justification, we must be able to set up an identity between eqns. (14) and (15). Testing this presumed identity is the subject of the rest of this section (3).

3.5. Concentration Properties of Empirical Coefficient A_2' - The identity between eqns. (14) and (15) may be simplified by writing:

$$A_2' = A_1' . p_o \tag{16a}$$

and so

$$R_s = k_1' . p_o \tag{16b}$$

whence, if the identity holds, the new empirical coefficient A_1' should now be independent of temperature and oxygen concentration, and dependent only upon velocity. This can be substantiated, in the first instance, by testing the relation of eqn. (16) against the experimental data. This can only be done for the two lower velocities, at 3.51 and 7.52 cm./sec., but the results, shown in Fig. 3 support the identity. For completeness, eqn. (16) has been assumed to hold for the other three velocities, even though measurements were made only at one oxygen concentration, and straight lines for these three velocities have also been included. The slopes of these lines give the empirical coefficients A_1', which should now be functions of velocity alone, with the temperature and concentration dependence eliminated.

3.5 Values and Properties of Empirical Coefficient A_1' - The variation of A_1' with velocity is shown graphically in Fig. 4; also shown, for reasons that will be developed, is its variation with $v_o^{1/2}$. This variation with the square root of the velocity follows from the identity between A_1' and k_1, which now reduces to

$$R_s = A_1' . p_o . \exp(-E_1'/RT) = B_1' . p_o . \exp(-E_1'/RT) \;/\; (1 + k_1/k_o) \tag{17a}$$

or

$$A_1' = B_1' \;/\; (1 + k_1/k_o) \tag{17b}$$

This formally incorporates the identification of E_1' in eqns. (8b) and (13) as being the same in both cases. It will be seen immediately from this that, if the adsorption rate is indeed very fast compared with the transport rate, k_o, then the ratio k_1/k_o would be large compared with unity, so we would get A_1' proportional to k_o: hence - from eqns. (2), (3), and (4) - to $v_o^{1/2}$. The significant curvature on the square-root plot of Fig. 4, substantiated by later plots, shows that k_1 is not very large compared with k_o. However, before these additional plots can be examined, one further point concerning the temperature dependence of the identity must be investigated.

3.6 Temperature Dependence of Empirical Coefficient A_1' - By the method of derivation, the coefficients A_2' and A_1' are necessarily defined as being temperature independent. It is apparent, however, from the proposed identity of eqn. (17b) that the right hand side of the identity still contains temperature-dependent terms. The coefficient B_1' is defined as being temperature independent; the dependency is incorporated solely in the two velocity constants, k_o and k_1. Since the two constnats appear in their ratio, k_1/k_o, what we must establish, for the identity not to fail, is that this ratio has negligible temperature dependence. From eqns. (2) and (8b) we can write:

$$k_o/k_1 = (A_o/B_1') . f \tag{18a}$$

where

$$f = (T/T_o)^{0.75}/\exp.(-E_1'/RT) \tag{18b}$$

the quantity, f, being the temperature function ratio. Taking E_1' as 2,000 cal. this temperature function ratio has been calculated out for the temperature range 900 to 1700°K, and the result of the calculation is shown graphically in Fig. 5. It is clear from this that the ratio is very constant indeed. For the range from 1000°K, the value of the ratio can be taken as 7.1 ± 0.1. This represents less than 1.5% variation which, compared with the scatter of the original experimental points, is quite acceptable. This confirms that the coefficient A_1' has now been reduced to a function of velocity alone.

3.7 Velocity Dependence of Empirical Coefficient A_1' - By using the temperature function ratio, f, of eqn. (18b), we may now re-write eqn. (17b) in the form:

$$1/A_1' = (1/B_1') + (1/fA_o) \qquad (19a)$$

or

$$= (1/B_1') + 1/f.K(2 + c'\sqrt{v_o}) \qquad (19b)$$

The only variable terms now left in this are: the independent variable of velocity, v_o; and the dependent variable, A_1', obtained by reduction from the experimental data. Eqn. (19) is not a function that can be tested directly as it stands but, as a first approximation, we may assume that 2 is small compared with $c'\sqrt{v_o}$. The appropriate plot to test this is given in Fig. 6, which like the square-root plot of Fig. 4, also shows detectable curvature. In point of fact, apparently good-fit straight lines could have been run through both plots but, when this was tried, there was then an inconsistency amounting to an order of magnitude in the values of the ordinate intercepts of the two plots. By successive approximation between the two plots to remove the inconsistency, an ordinate intercept in Fig. 6 of value 100 was finally adopted for the quantity $1/B_1'$. This value was then used to test the following final arrangement of eqn. (19b):

$$1/\left[(1/A_1') - (1/B_1')\right] = 2fK + (fKc')\sqrt{v_o} \qquad (19c)$$

This final equation was tested by the plot of Fig. 7. This shows that the function is satisfactorily obeyed with an intercept of value 0.6×10^{-3}, this being the value of the quantity (2fK).

This functional agreement thus substantiated the identity of the empirical coefficient A_1' with the theoretical quantity $B_1'/(1 + k_1/k_o)$, as in eqn. (17b).

3.8 Coefficient Values - What we have now established is that the proposed equations have the correct functional form, which therefore provides qualtative substantiation of the picture developed. However, the graphical plots do more than this: they also provide experimental values, by way of slopes and intercepts, of the various coefficients involved, and these experimental values can now be compared with the values predicted from theory. In general, these will be seen to show agreement between prediction and experiment that varies from adequate to excellent.

3.8.1 Diffusion and Velocity Coefficients - (i) Zero velocity: At zero velocity, we get the limiting value of 2 for the Nusselt number. Physically, this represents the situation where the particle is surrounded by a totally quiescent diffusion film exerting its maximum influence. To compare theory and experiment, the experimental coefficient relating to zero velocity is the ordinate intercept on Fig. 7. From this plot, this intercept has the value: 0.6×10^{-3}. By eqn. (19c), this value is predicted by the quantity (2fK); i.e., $2f(\rho_o M_c/M_o)(D_o/d)$. Taking the following values for these quantities: ρ_o as 1.43×10^{-3} g/c.c.; M_c and M_o as 12 and 32 respectively; D_o as 0.181 sq. cm./sec.; and d as 2.54 cm.; we have $K = 3.83 \times 10^{-5}$. Since f, from Fig. 5, has the value 7.1, we also have

predicted value: $2fK = 14.2 \times 3.83 \times 10^{-5}$

$= \underline{0.545 \times 10^{-3}}$ compared with

experimental value: $= \underline{0.60 \times 10^{-3}}$

This agreement is clearly acceptable. It is, however, no more than we now expect from diffusion calculations in view of the excellent agreement already obtained elsewhere (15-17) using such calculations. Confidence in the accuracy of diffusion calculations is now very high.

(ii) Finite velocity: In the following system, the agreement on coefficients is as good, though the order of agreement depends on whose equation is chosen from the literature for comparison of the coefficients; there are also two points that can be queried about the method of the theoretical calculation. To compare theory and experiment, we have in this instance the comparison of the values for the slope of Fig. 7. The experimental value, from the plot, is 0.725×10^{3}. The predicted value is given, again from eqn. (19c), by its second term, as: fKc'. The value of fK is given above as 0.2125×10^{-3}; and for c' is given (from Ranz and Marshall's data (22)) under eqn. (4b) as 2.64. Hence we have:

predicted value: $fKc' = 0.2125 \times 10^{-3} \times 2.64$

$= \underline{0.7175 \times 10^{-3}}$ compared with

experimental value: $= \underline{0.725 \times 10^{-3}}$

This agreement is also excellent. The only reservations on the predicted value are concerned with: the use of the s.t.p. gas viscosity in evaluation of the c' coefficient (in eqn. 4b). Since the gas viscosity increases roughly in proportion to the square root of the temperature then, taking a mean temperature of 1500°K, the correction factor to be applied is division by the fourth root of 1500/273. This gives us about 1.5. However, we should also correct for the increased velocity past the sphere at its perpendicular diameter to the gas flow due to the constriction of the tube. This gives us a multiplying correction factor, for both corrections combined, of about 0.75. If, however, we then use Khitrins coefficient of 0.7 (23), instead of Ranz and Marshall's of 0.6 (22), the correction factor is about 0.9. This would still put the agreement between the predicted and experimental values within an acceptable 10%, but quite clearly, the possibilities of selecting values that will fit becomes so wide that better agreement finally becomes meaningless.

3.8.2 High Temperature Rate Coefficients - (i) Energy of Activation, E_1: The choice of apparent energy of activation, E_1, has been fully discussed above. This is not a quantity that can easily be predicted from first principles. A few have been (e.g.: adsorption of H_2 on carbon (37)), but no simple general method yet exists.

The apparent value is related to the true value by eqn. (8). The effect of dividing the Arrhenius exponential by $\sqrt{T/T_0}$ is to reduce the true value by about 1400 cal. By calculating the quantity $\exp(-E_1'/RT) \times \sqrt{T/T_0}$, and making an Arrhenius plot, a value of 3,400 cal. was obtained for the true activation energy E_1. This is clearly in line with the values given by Blyholder and Eyring (30), and by Barrer (32) for low area of coverage; it is also in line with the estimates made elsewhere (2). Another interesting figure can be extracted from the low temperature and pressure studies of Laine, Vastola, and Walker (38). They quote activation energies of 44,000 cal. for carbon gasification with oxygen, and 36,000 cal. for the simultaneous oxygen depletion. As with Gulbransen and Andrew (39) (whose respectove figures were: 40,000 and 35,000 cal.), these represent respectively the values for the desorption process alone, and for the total reaction. If the latter figure is the value of $(E_2 - E_1)$, then we have a subtraction, values for E_1 of 8,000 and 5,000 cal.

from Laine et al. and Gulbransen and Andrew respectively. Both figures are in line with Barrer's values (32) at low to medium coverage, and the higher is close to Bannerjee and Sarjants value (40) of 8,300 cal.

(ii) Frequency factor: This is the quantity A_1, or B_1 as the temperature-independent form of the coefficient, given theoretically by eqn. (7). It is related to the experimental quantity, B_1', through eqns. (7) and (8). The experimental value of B_1' is 0.01, obtained as described in sec. 3.7 by successive approximation. By eqn. (8) we get, for B_1, a value of 0.039. This, however, is substantially lower than the predicted value of B_1 when the orientation coefficient is unity. Taking P as 1.013×10^6 dynes/sq. cm.; M as 30; and R as 8.37 ergs/degree mole; we get a calculated value of 5.89 for B_1. Since this is substantially above the experimental value of B_1, we may reasonably infer, following Laine et al. (38), that the difference is due to the orientation or steric factor, η. This can be calculated from the identity:

$$\eta = B_1(\text{exptl.})/B_1 \ (\text{predtd.})$$

$$= 0.039/5.88$$

$$= 1/150$$

This is witin a factor of 2 or 3 of the values for η given by Laine et al. (38), which ranged from 1/56 to 1/83. If the adduced explanation for the discrepancy between the two B_1 values is correct, the values of are at least in order of magnitude agreement.

3.8.3 Low Temperature Rate Coefficients - Little need be said about the low temperature coefficients. The identification and interpretation of these has never been in dispute. The values of A_2 and E_2 adopted, as described above, of respectively: 1.05×10^4 g/sq.cm.sec., and 40,000 cal., are in line with other values given in original papers and reviews, to which reference may be made for comparison.

4. DISCUSSION

4.1 General - What these results clearly establish, to our mind, are: first, the general validity of the approach; second, substantiation of the high reliance that may be placed on the diffusion calculations; and, third, the degree of confidence to which the quoted equations may be used for calculating mass transfer in a flowing system. Given these, the most important final conclusion that may be drawn is the relative importance of the high-temperature resistance, S_1, in comparison with the diffusional resistance, S_o. This final point is now amplified in the sections following.

4.2 Resistance Ratios - (i) S_1/S_o: To show the relative importance of S_1 to S_o, which former has hiterto been generally neglected as too small, Fig. 8 shows a plot of their ratio as a function of velocity. The single line given is valid over the temperature range 1100 to 1700°K, to within about 1%; it is also independent of oxygen concentration. This shows that, over the velocity range of the experiments, the resistance ratio rises from 0.18 to 0.57. As percentages of the total reaction resistance, these figures show that S_1 rises from 15% to 36%, which clearly is not negligible. This confirms the conclusion drawn from eqn. (11) that continuity in the slopes of the curves can only mean that S_1 is significant.

At zero velocity, the ratio does become very small, dropping to about 20:1. This however, is true only for these very large spheres. Since S_o is proportional to the sphere diameter, d, by eqns. (10), (2), and (3), we then have that the resistance ratio is inversely proportional to the diameter, d. Thus,

even in a quiescent system, reduction of d from one inch to 2.5 mm would raise the resistance ratio up to 2 to 1: i.e., the two would be comparable in value. At 250 microns, the ratio goes to 20 to 1 in favour of the chemical resistance; and at 25 microns, or pulverised coal particle size, the diffusional resistance, S_o, becomes totally unimportant, in agreement with previous predictions and calculations (41,42) (also see below).

If, on the other hand, the high temperature frequency factor, A_1 ever attained its full theoretical value, the S_1 resistance would not become important till the particle size dropped below 100 microns. Above this, it would not matter. This may well have been the case for the carbons formed in situ from burning coal particles since no evidence of a chemical resistance was ever found (15-17) for particles ranging in size as low as 300 microns. This suggests that A_1 may depend as much on the inherent reactivity of the material as it does on any accomodation or orientation factor.

(ii) S_1/S_2: This alternative plot is shown in Fig. 9. In this instance the two resistances are independent of velocity, but are very strongly influenced by temperature and oxygen concentration. Even so, the two resistances are equal, over the range 5 to 21% oxygen, at a temperature of around 1200 ± 100°K; and there is substantially change from S_2 control to S_1 control (if S_o is absent) in the temperature range 1200°K ± 200°. For the 1" spheres, inspection of Fig. 2 indicates a transition temperature of about 1000°K ± 200° (cf. data in Review (3)), thus implying a surface oxygen concentration (p_s) of 1% or less. Since the oxygen concentrations can be read as surface values (i.e., of p_s), rather than main stream values, the progressive reduction of the diffusion layer, due to a rising velocity, or falling particle size, is seen to increase the surface oxygen concentration, and to raise the transition temperature.

4.3 Small Particle Behavior and Other Data - As mentioned above, the diffusion resistance, S_o, becomes neglible as the particle size drops below 100 microns. Small particle behavior, as in pulverised coal flames (9), or soot particles in cracked hydrocarbon flames (10), can therefore be evaluated from eqn. (10) and Fig. 9. According to these, we should find that, even in the most favorable conditions for the resistance S_2, the S_1 resistance should predominate above 1400°K. Data (9,10), however, show that high activation energies, of about 40,000 cal., can be adduced over the range 1300 to 1700°K. This, of course, is quite feasible if the S_1 value for particles formed from coal in situ can indeed drop by a factor of 10^2, as discussed above. At 5% oxygen concentration, the S_2 resistance would not drop below 10% of the total resistance till the temperature exceeded 1900°K.

Such behavior would satisfactorily account for the results obtained, except that both reactions are claimed to be first order. A possible reason for this further discrepancy may be that there is even a fourth resistance or mechanism coming into play at the higher temperatures. Smith and Gudmundsen (43) measured burning rates of small spheres, 2 or 3 mm in diameter, at temperatures ranging from 1450 to 1750°K. At the lower temperatures in this range, the reaction rates obtained substantially agree with prediction from the equations developed in this paper, using the same experimental coefficients. The initial slopes of the curves with respect to temperature are also similar; but above 1650°K, where Tu et al. had very few data, the slopes of the Smith and Gudmundsen curves increase very rapidly indeed, with the activation energy evidently high. Golovina and Khaustovich (24) have shown the same effect, also using spheres of very similar diameter to those used by Tu (of 1.5 cm.) and in a 60 cm./sec. air flow. In agreement with Tu, the reaction rates rose fast up to 1000 or 1100°K, then levelling off at about 30 x 10^{-5} g./sq.cm.sec.

(cf. Fig. 3). Then, in agreement with Smith and Gudmundsen, they rose fast again over the temperature range 1400 to 1750°K, rising to about 70×10^{-5} g./sq.cm.sec.; but then they levelled off again, with calculated rates in agreement with a double film diffusion system, this being maintained up to the experimentalltemperature limit of 3000°K.

This phenomenon shown by Smith and Gudmundsen (43) and by Golovina and Khaustovich (24) in the temperature range 1500 to 1700°K may, therefore account for the Lee et al. (10) anomalies, but clearly this is a region now requiring examination, both theoretically and experimentally in much greater detail.

5. CONCLUSIONS

From this analysis, of the Tu, Davis, and Hottel data (1), on the burning rates of 1" carbon spheres, presented in this paper, we conclude that:

1. The three-resistance concept of: boundary-layer diffusion (S_o), activated adsorption (S_1), and desorption (S_2), which are deemed to take place physically in series, is essentially correct.

2. At low temperatures (below 1000°K) the desorption resistance (S_2) predominates, and the reaction order is zero. At high temperatures, (above 1000°K), the diffusion and adsorption resistances (S_o and S_1) are both, simultaneously important, and the reaction is first order. For the 1" sphere at low velocities, S_1 is the lower of the two resistances, being 1/6 of S_o at 3.5 cm./sec. gas velocity; but rising to 1/2 of S_o at 50 cm./sec.

3. At higher velocities, or smaller particle sizes, the diffusion resistance, S_o, becomes progressively less important. In general, it should be possible to neglect it with little error, at particle sizes less than 100 microns (pulverised coal size), even in quiescent ambient gas conditions.

4. The reciprocal of the three resistances are related to the velocity constants of the three precosses, given generally by:

$$1/S_o = k_o p_o = A_o . p_o . (T/T_o)^{0.75}$$

$$1/S_1 = k_1 p_o = A_1 . p_o . \exp(-E_1/RT) = B_1' . p_o . \exp(-E_1'/RT)$$

$$1/S_2 = k_2 = A_2 . \exp(-E_2/RT)$$

the coefficients A_o, A_1, And B_1' being given by eqns. (3) and (7). A_o is velocity dependent, and temperature independent; A_1 is temperature dependent, and velocity independent; and B_1' and A_2 are both temperature and velocity independent.

5. The relation between specific reaction rate (R_s) and the velocity constants is given by the quadratic of eqn. (9) However, the data may be approximated by the modified Langmuir isotherm.

$$1/R_s = (1/k_1' . p_o) + (1/k_2)$$

where $$k_1' = A_1' . \exp(E_1'/RT)$$

A_1' and E_1' are empirical quantities determined by experiment. A_1', by definition, is independent of both temperature and oxygen concentration, but is velocity dependent.

6. The empirical activation energy, E_1', is identified with the effective activation energy, obtained from first principles, after combining the $T^{1/2}$ term of A_1 with the E_1 term in S_1 (E_1 being the true activation energy). The value of the effective energy, E_1', is found by best fit to experiment to have a value of 2000 cal./mole. By calculation from this, the true value, E_1, is 3400 cal./mole, in adequate agreement with other values for this quantity in the literature.

7. The empirical frequency factor, A_1', is identified with the theoretical group obtained from first principles:

$$A_1' = B_1' / (1 + k_1/k_o) \qquad (17b)$$

From this, the following relation with velocity is obtained:

$$1/[(1/A_1') - (1/B_1')] = 2fK + fKc'\sqrt{v_o} \qquad (19c)$$

Comparison with experiment confirmed the functional form of this equation; and excellent agreement was found between the predicted and experimental coefficients involved in the diffusion and velocity components of the calculation.

8. Agreement between the predicted and experimental values of the A_1 and B_1 frequency factors are in error by a factor of 150. This is attributed to an orientation or steric factor, ϵ, for which other values in the literature are in the range of 50 to 80. For this identification, agreement is therefore adequate.

9. A final point developing from this analysis is an ambiguity or inconsistency in higher temperature data, obtained by others, that just overlap in their bottom ranges with the top temperature range of those obtained by Tu et al. In the overlap, the data agree; but at higher temperatures, beyond the overlap, the data show a much more rapid risein reaction rate than the equations and mechanism should permit. This phenomenon requires further study.

6. LIST OF SYMBOLS

A - frequency factor
A_o - " " for diffusion = $K.Nu$
A_1 - " " for adsorption = $M_c P\eta / \sqrt{2\pi MRT}$
A_2 - " " for desorption
A_1' - first empirical factor = $B_1' / (1 + k_1/k_o)$
A_2 - second empirical factor = $A_1' p_o$
b - conversion factor (numerical) in $B_1 = b.B_1'$: value 3.9
B_1 - adsorption frequency factor (temp. indep.) = $A_1 . \sqrt{T/T_o}$
B_1' - effective adsorption frequency factor = B_1/b
c - numerical constant in Nusselt/Reynolds No. equation
c' - revised value of c for velocity equation = $c\sqrt{\rho_o d/\mu}$
d - particle diameter (this paper = 2.5 cm.)
D_o - diffusion coefficient at s.t.p. (for O_2 in N_2 = 0.181)
E_1 - adsorption activation energy (true) = 3400 cal/mole
E_1' - empirical and effective adsorption activation energies = 2000 cal./mole
E_2 - desorption activation energy (true) = 40,000 cal./mole
f - temperature function ratio: $(T/T_o)^{0.75}/\exp(-E_1'/RT)$: value = 7.1
k - velocity constant
k_o - velocity constant for diffusion = $A_o(T/T_o)^{0.75}$

k_1 - velocity constant for adsorption = $A_1.\exp(-E_1/RT)$
k_2 - " " for desorption = $A_2.\exp(-E_2/RT)$
k_1' - first empirical velocity constant
k_2' - second empirical velocity constant = $k_1' p_o$
K - diffusional constant group = $(\rho_c M_c/M_o)\ (D_o/d)$
m) - general indices, for Re and Pr numbers
n)
M_c - molecular weight of carbon
M_o - molecular weight of oxygen
Nu - Nusselt number for mass transfer
p_o - oxygen partial pressure, main stream value
p_s - oxygen partial pressure, solid surface value
P - total pressure (1 atmos.)
Pr - Prandtl number
Re - Reynolds number
R_s - specific reaction rate - g/sq.cm.sec.
S_o - diffusional resistance = $1/k_o p_o$
S_1 - adsorption resistance = $1/k_1 p_o$
S_2 - desorption resistance = $1/k_2$
T - temperature (absolute)
T_o - s.t.
V_o - s.t.p. gas velocity
ρ_o - s.t.p. density
η - orientation or steric factor in adsorption
μ - gas viscosity

7. REFERENCES

1. Tu, C.M.; Davis, H.; and Hottel, H.C. Ind. Eng. Chem. 26, (1934) 749.
2. Essenhigh, R.H. Sheffield Univ. Fuel Soc. J. 6 (1955) 15.
3. Essenhigh, R.H. and Perry, M.G. Introductory Survey "Combustion and Gasification", Proc. Conf. "Science in the Use of Coal", Sheffield, 1958, p. D1: Institute of Fuel, London, 1958.
4. Walker, P.L., Rusinko, F. and Austin, L.G. Advances in Catalysis, Vol. II, pp. 134-221, Academic Press Inc., New York 1959.
5. Thring, M.W. and Essenhigh, R.H. "Chemistry of Coal Utilization": Supplementary Volume ch. 17, pp. 754-772, Wiley; New York, 1963.
6. Brunauer, S. "Adsorption of Gases and Vapors, p. 10, Oxford University Press, 1945.
7. Fischbeck, K.Z. Electrochem 39 (1933) 316; 40 (1934) 517.
8. Hottel, H.C. and Stewart, I.M. Ind. Eng. Chem. 32 (1940) 719.
9. Beer, J.M. and Thring, M.W. 1960 Anthracite Conference Proceedings: M. I. Experiment Station Bulletion No. 75 (Sept. 1961) p. 25 Pennsylvania State University.
10. Lee, K.B., Thring, M.W. and Beer, J.M. Combustion and Flame 6, (1962) 137.
11. Godsave, G.A.E. Nat. Gas Turbine Estab. Report No. R.126 (1952).
12. Spalding, D.B. Proc. Inst. Mech. Engrs. (Lond) 168 (1954) 545.
13. Noyes, A. and Whitney, K. Z. phys. Chem. 23 (1897) 689.
14. Nusselt, W. V.D.I. 68 (1924) 124.
15. Essenhigh, R.H. and Thring, M.W. Inst. Fuel Conference "Science in the Use of Coal", Sheffield, April 1958, Paper 28, p. D21. Inst. Fuel (London) 1958.
16. Essenhigh, R.H. J. Engrg. for Power, 85 (1963) 183.
17. Beeston, G. and Essenhigh, R.H. J. Phys. Chem. 67 (1963) 1349.

18. Sherwood, T.K. and Pigford, R.L. "Adsorption and Extraction", p.2, New York 1952.
19. International Critical Tables 5 (1929) 62.
20. Grober, H. and Erk, S. "Fundamentals of Heat Transfer", pp. 282, 283, 4.2, 3rd ed. (trans.) McGraw Hill 1961.
21. Frank-Kamenetskii, D.A. "Diffusion and Heat Exchange in Chemical Kinetics" Ch I and II: Princeton Univ. Press (Trans.) 1955
22. Ranz, W.E. and Marshall, W.R. Chem. Eng. Prog. 48 (1952) 403.
23. Predvoditelev, A.S., Khitrin, L.N., Tsukhanova, D.A., Colodtsev, H.L. and Grodzovski, M.K. Gorenic Ugleroda (1949), Izdatelstvo AN SSSR.
24. Golovina, E.S. and Khanstovich, G.P. 8th International Combustion Symposium (1960) Paper 84, p. 784, Williams and Wilkins Co., Baltimore 1962.
25. Graham, J.A., Brown, A.R.G., Hall, A.R. and Watt, W. Conf. on Ind. Carbon and Graphite, Soc. Chem. Ind. (Sept.) 1957.
26. Day, R.J. Ph.D. Thesis, The Pennsylvania State University, 1949.
27. Essenhigh, R.H. and Fells, I. Faraday Soc. Discussions "The Physical Chemistry of Arosols" (Bristol 1960), p. 208, Faraday Soc. 1961.
28. Gadsby, J., Long, F.J., Sleightholm, P. and Sykes, K.W. Proc. Roy. Soc. A193 (1948) 357.
29. Gadsby, J., Hin shelwood, C.N. and Sykes, K.W. Proc. Roy. Soc. A187 (1946) 129.
30. Blyholder, G.D. and Eyring, H. U.S. Air Force: Office of Scientific Research Report (Technical Note) O.A. NoXX August 1956.
31. Trapnell, B.M.W. "Chemisorption", pp. 70,71, Butterworths Scientific Publications (London) 1955.
32. Barrer, R.M. J. Chem. Soc. (1936) 1261.
33. Parker, A.S. and Hottel, H.C. Ind. Eng. Chem. 28 (1936) 1334 - Analysis by D.A. Frank-Kamenetskii, (ref. 62 to 64.
34. Arthur, J.R. and Bleach, J.A. Ind. Eng. Chem. 44 (1952) 1028.
35. Barrer, R.M. and Rideal, E.K. Proc. Roy Soc. A149 (1935) 231, 253.
36. Wicke, E. 5th Internation Sumposium on Combustion 1955, paper 17, p. 245 (Reinhold Pub. Corp. 1956).
37. Sherman, A. and Eying, H. J. Am. Chem. Soc. 54 (1932) 2661.
38. Laine, N.R., Vastola, F.J. and Walker, P.L. J. Phys. Chem. 67 (1963) 2030.
39. Gulbransen, E.A. and Andrew, K.F. Ind. Eng. Chem. 44 (1952) 1034, 1039, 1048.
40. Bannerjee, S. and Sarjant, R.J. Fuel 30 (1951) 130.
41. Beer, J. M. and Essenhigh, R.H. Nature (London) 187 (1960) 1106.
42. Essenhigh, R.H. J. Inst. Fuel, 34 (1961) 239.
43. Smith, D.F. and Gudmundsen, A. Ind. Eng. Chem. 23 (1931) 277.

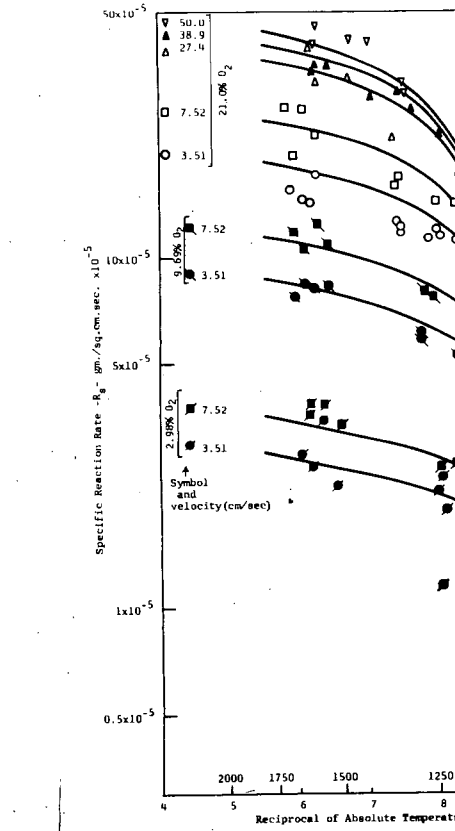

Figure 1 - Data Plot - Original data from Tu, Davis, and Hottel[1]
Arrhenius plot, showing agreement with calculated curves (full lines) according to equation (9) (see text) of: Specific reaction rate (R_s) against reciprocal of temperature (1/T).

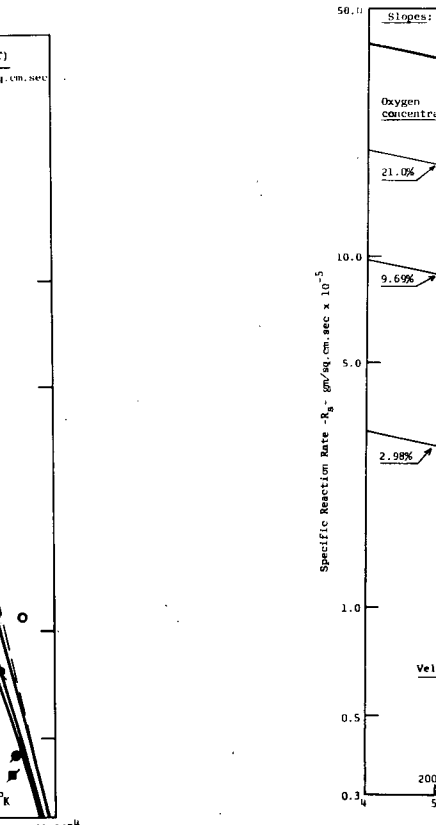

Figure 2 - Fitting Plot. Curves drawn according to equation: $1/R_s = (1/k_2') + (1/k_2)$. Data from Tu, Davis, and Hottel[1]

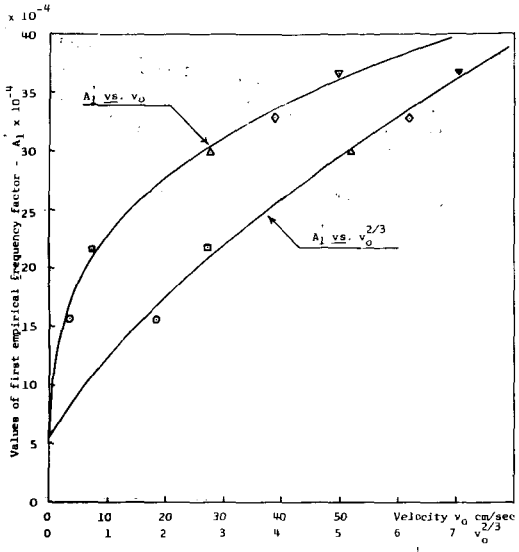

Figure 4 - Plot of first empirical frequency factor (A_1') against: (1) Velocity (v_o); (2) Square-root velocity ($v_o^{2/3}$)
Data: Derived from Tu, Davis, and Hottel[1]

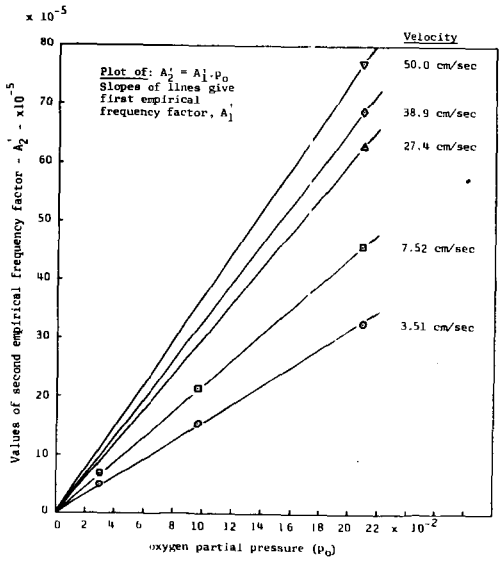

Figure 3 - Plot of second empirical frequency factor (A_2') against oxygen partial pressure (p_o), to show linear relationship - for two lower velocities. Three higher velocities (27.4, 38.9, and 50.0) added for comparison.
Data: Derived from Tu, Davis, and Hottel[1]

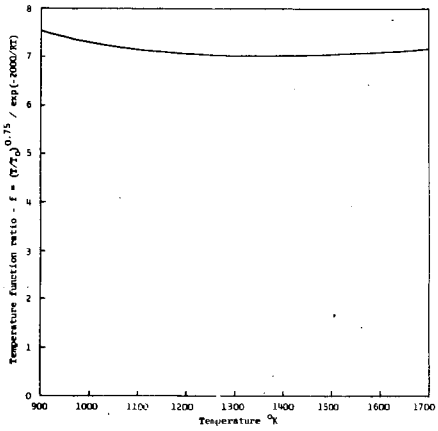

Figure 5 - Plot of temperature function ratio (f) against temperature (T) to show the constancy of 'f' with 'T'.

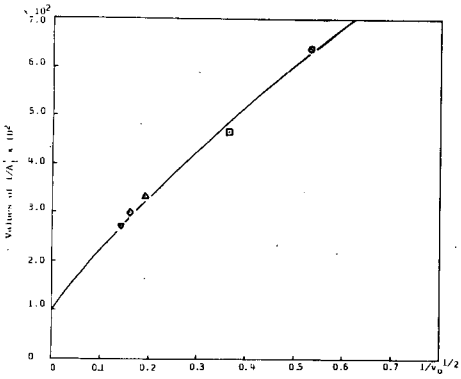

Figure 6 - Plot of reciprocal of first empirical frequency factor $(1/A_1')$ against reciprocal of square-root of velocity $(1/v_o^{1/2})$
Data: Derived from Tu, Davis, and Hottel (1)

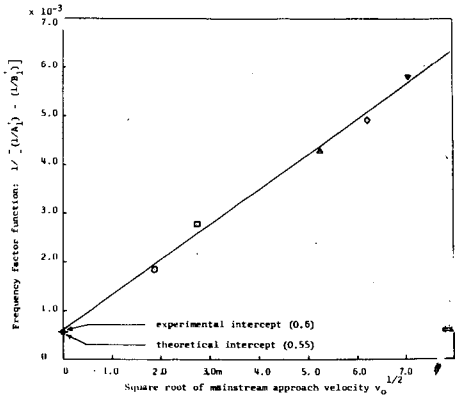

Fig 7 - Test of eqn. (19c). Plot of Frequency factor function against square root of velocity $(v_o^{1/2})$
Data: Derived from Tu, Davis, and Hottel

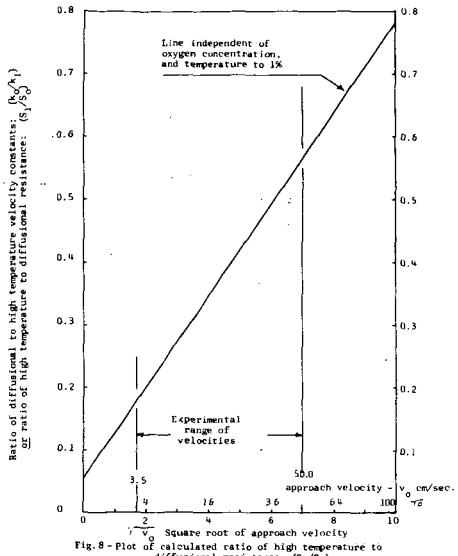

Fig. 8 - Plot of calculated ratio of high temperature to diffusional resistance (S_1/S_D) against velocity (v_o and $\sqrt{v_o}$)

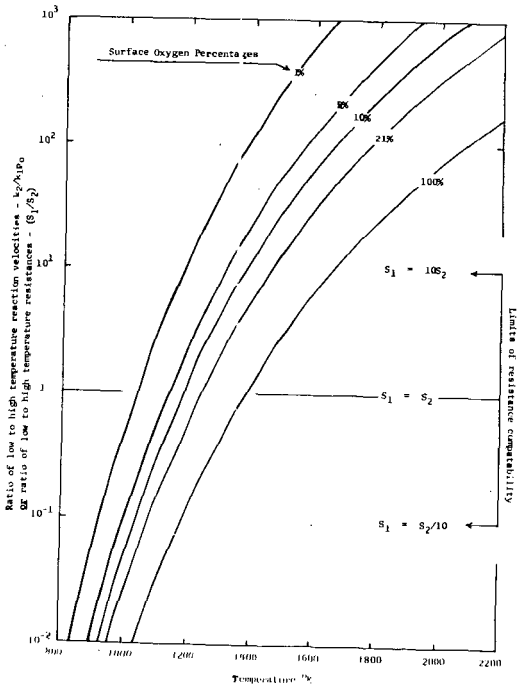

Figure 9 - Plot of calculated ratio of high to low temperature resistances (S_1/S_2), as a function of temperature, for S levels of oxygen concentration.

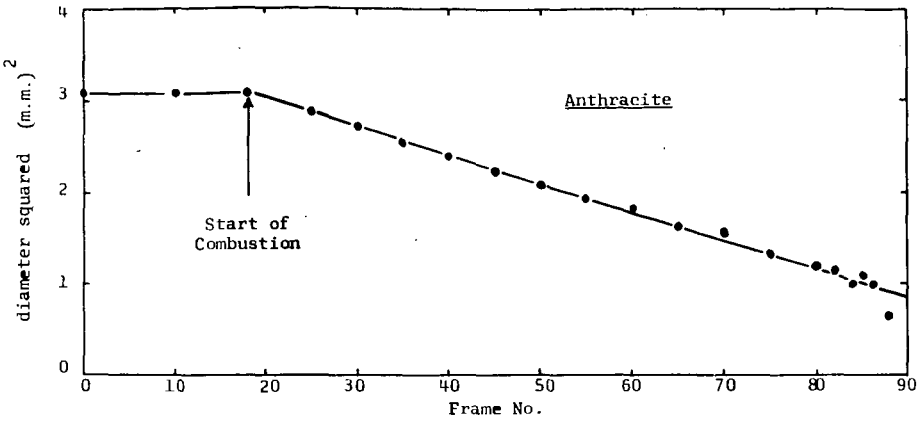

Figure 1 - Variation of diameter squared with time of burning anthracite particle (Stanllyd)

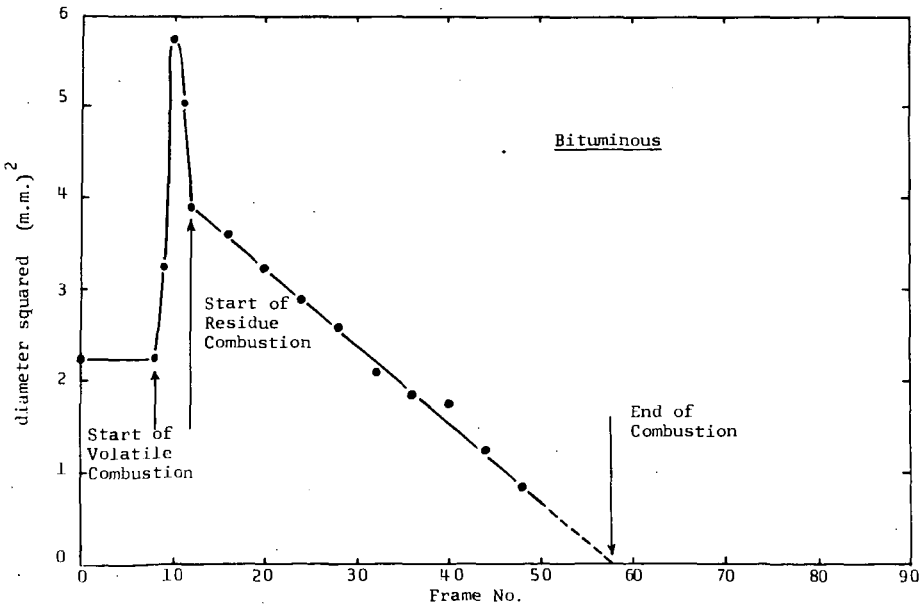

Figure 2 - Variation of diameter-squared with time of burning bituminous coal particle (Cowpen)